Nanoscale Research Letters

Involvement of ubiquitin-editing protein A20 in modulating inflammation in rat cochlea associated with silver nanoparticles-induced CD68 up-regulation and TLR4 activation
--Manuscript Draft--

Manuscript Number:	NARL-D-16-00191R1
Full Title:	Involvement of ubiquitin-editing protein A20 in modulating inflammation in rat cochlea associated with silver nanoparticles-induced CD68 up-regulation and TLR4 activation
Article Type:	Nano Express
Funding Information:	Seventh Framework Programme (263147) / Prof. Ilmari Pyykkö

Abstract:	AgNPs were shown to temporarily impair the biological barriers in the skin of the external ear canal, mucosa of the middle ear, and inner ear, causing partially reversible hearing loss after delivery into the middle ear. The current study aimed to elucidate the molecular mechanism, emphasizing the TLR signaling pathways in association with the potential recruitment of macrophages in the cochlea and the modulation of inflammation by ubiquitin-editing protein A20. Molecules potentially involved in these signaling pathways were thoroughly analysed using immunohistochemistry in the rat cochlea exposed to AgNPs at various concentrations through intratympanic injection. The results showed that 0.4 % AgNPs but not 0.02 % AgNPs, up-regulated the expressions of CD68, TLR4, MCP1, A20, and RNF11 in the strial basal cells, spiral ligament fibrocytes, and non-sensory supporting cells of Corti's organ. 0.4 % AgNPs had no effect on CD44, TLR2, MCP2, Rac1, myosin light chain, VCAM1, Erk1/2, JNK, p38, IL-1β, TNF-α, TNFR1, TNFR2, IL-10, or TGF-β. This study suggested that AgNPs might confer macrophage-like functions on the strial basal cells and spiral ligament fibrocytes and enhance the immune activities of non-sensory supporting cells of Corti's organ through the up-regulation of CD68, which might be involved in TLR4 activation. A20 and RNF11 played roles in maintaining cochlear homeostasis via negative regulation of the expressions of inflammatory cytokines.

Corresponding Author:	Jing Zou, M.D., Ph.D. University of Tampere, School of Medicine Tampere, FINLAND
Corresponding Author Secondary Information:	
Corresponding Author's Institution:	University of Tampere, School of Medicine
Corresponding Author's Secondary Institution:	
First Author:	Hao Feng
First Author Secondary Information:	
Order of Authors:	Hao Feng
	Ilmari Pyykkö
	Jing Zou, M.D., Ph.D.
Order of Authors Secondary Information:	

Response to Reviewers:	Dear Editor-in-Chief, I have revised our manuscript entitled 'Involvement of ubiquitin-editing protein A20 in modulating inflammation in rat cochlea associated with silver nanoparticles-induced CD68 up-regulation and TLR4 activation (NARL-D-16-00191)' according to the reviewer's comments. Details on the response are shown below: 1. The toxicity of AgNPs was usually related to the particle size and surface properties. The paper lack of data about the characterization of AgNPs. The authors had better to provide more detailed data, such as TEM, DLS, UV-Vis, zeta potential, etc. Reply: The characterization of AgNPs was shown in our previous study that has been

cited in the revised manuscript (P6, L6-10).

2. The authors should state how they selected the exposure concentrations of AgNPs for the experiment.
Reply: More details have been included (P6, L15-20).

3. The release of Ag ions from AgNPs is considered an important mechanism of AgNPs-induced toxicity. So in this study, the exact mechanism of AgNPs-induced biological barrier functional changes in the inner ear was depended on Ag ions or AgNPs particle effect, please provide the results.
Reply: More details have been included (P17, L8-15).

The revised text mentioned above is highlighted in yellow shadow in the main manuscript.

Thank you for considering the enclosed revised report for publication in Nanoscale Research Letters.

Sincerely yours,

Jing Zou
M.D., Ph.D., Associate Professor
Head of Hearing and Balance Research Unit
Field of Oto-laryngology, School of Medicine, University of Tampere
Room C2165, Medisiinarinkatu 3, 33520
Tampere, Finland
Tel.: +358 40 190 1307
Fax: +358 3364 1482
E-mail: Jing.Zou@staff.uta.fi

Involvement of ubiquitin-editing protein A20 in modulating inflammation in rat cochlea associated with silver nanoparticles-induced CD68 up-regulation and TLR4 activation

Hao Feng[1], Ilmari Pyykkö[1], Jing Zou[1, 2, *]

[1]Hearing and Balance Research Unit, Field of Oto-laryngology, School of Medicine, University of Tampere, Tampere, Finland

[2]Department of Otolaryngology-Head and Neck Surgery, Center for Otolaryngology-Head and Neck Surgery of Chinese PLA, Changhai Hospital, Second Military Medical University, Shanghai, China

[*]Correspondence: Jing Zou

Hearing and Balance Research Unit, Field of Oto-laryngology

School of Medicine, University of Tampere

Medisiinarinkatu 3

33520 Tampere, Finland

Tel.: +358 40 190 1307

Fax: +358 3364 1482

E-mail: zoujinghb@hotmail.com, Jing.Zou@staff.uta.fi

Background

With the rapid development of nanotechnology and increasing applications of engineered nanomaterials in our daily lives, their potential safety issues have become a serious concern in public health. The rat ear model has been applied to investigate the impact of silver nanoparticles (AgNPs) on the permeability of biological barriers in the skin, mucosa, and inner ear that is analogous to the nervous system (*e.g.*, brain and spinal cord) [1]. Previous research showed that AgNPs led to hyaluronan accumulation in the cochlea, impaired biological barriers in the skin of the external ear canal, mucosa of the middle ear, and inner ear, and consequently caused hearing loss after delivery into the middle ear [1-3]. Hyaluronan acts as an endogenous pathogen-associated molecular pattern (PAMP) in response to hazardous signals through binding to hyaluronan binding proteins (hyaladherins) including toll-like receptors 2/4 (TLR2/4), CD44, receptor for hyaluronan-mediated motility, and tumour necrosis factor-α (TNF-α)-stimulated glycoprotein-6 [4-7]. Among them, TLR2/4 are a category of mammalian homologues of *Drosophila* Toll proteins that are of great importance for innate host defence. They belong to the pattern recognition receptors (PRRs) that specifically recognize and respond to an expansive variety of PAMPs [8]. Moreover, TLR4 is responsible for sensing danger/damage-associated molecular patterns (DAMPs) and conferring immunostimulatory activity [9]. The activation of TLRs initiates the up-regulation of transcription factors [*e.g.*, nuclear factor-κB (NF-κB) and activator protein-1] that play pivotal roles in producing inflammatory molecules [*e.g.*, interleukin-1β (IL-1β), interleukin-6 (IL-6), and TNF-α together with its receptors TNFRs], chemokines (*e.g.*, monocyte chemoattractant proteins, MCPs), and reactive oxygen/nitrogen species, leading to inflammatory diseases [10-12].

1 Several proteins that are implicated in mediating TLR signaling attenuation have been identi-

2 fied such as the ubiquitin-editing protein A20 [13-15]. A20 acts as a negative effector in regu-

3 lating TLR-mediated inflammatory response, and its over-expression inhibits TLR2- and

4 TLR4-mediated IL-8 synthesis in airway epithelial cells [16]. A20 loss elevates the levels of

5 NF-κB-regulated inflammatory cytokines and causes spontaneous cerebral inflammation [17].

6 RING finger protein 11 (RNF11), a critical component of A20, is indicated as one of the key

7 negative regulators in controlling the NF-κB signaling pathway. RNF11 was shown to protect

8 microglia irritated by lipopolysaccharide through manipulating the NF-κB signaling pathway

9 [18]. RNF11 knockdown in the monocytes led to persistent TNF- and lipopolysaccharide-me-

10 diated NF-κB signaling activation and up-regulated NF-κB-associated inflammatory gene tran-

11 scripts [18, 19].

12

13 As another important hyaladherin, CD44 is capable of recruiting monocytes from the peripheral

14 blood upon hyaluronan binding [20]. Further study has revealed that weakened interaction be-

15 tween CD44 and hyaluronan decreases the production of MCPs and consequently undermines

16 the recruitment of mononuclear cells [21]. MCPs are a family of small heparin-binding, posi-

17 tively charged chemokines that play an indispensable role in controlling cell behaviour in re-

18 sponse to exogenous stimulation. They are crucial in triggering the mobilization and migration

19 of immunocompetent cells such as monocytes, neutrophils, lymphocytes, and dendritic cells

20 along bone marrow sinusoids that frequently anastomose with capillaries and in directing them

21 into the inflamed tissues [22]. In the inner ear, spiral ligament fibrocytes act as the primary

immune sensors in response to lipopolysaccharide, involving TLR2-dependent NF-κB signaling activation and MCP1 up-regulation and resulting in monocyte migration and consequential infiltration [23, 24].

Adhesion molecules play a critical role in mediating leukocyte immobilization as a result of anchoring [25]. Among them, vascular cell adhesion molecule 1 (VCAM1) enables rolling monocytes along the microvascular wall at a far slower velocity to adhere to the endothelial cells [26]. Rac1, a member of Rho-like small GTPase, mediated by the phosphorylation of myosin light chain protein, facilitates actin cytoskeletal remodelling and modulates tight junctional proteins (*e.g.*, occludin and claudin). The breakdown of tight junction in the microvascular wall enables the leukocytes to infiltrate into the targeting site [27-29]. The extracellular signal-regulated kinases 1/2 (Erk1/2), c-Jun N-terminal kinases 1/2/3 (JNK1/2/3, also known as stress-activated protein kinases), and p38 isoforms (α, β, γ, and δ) that belong to the MAPKs family are considered to be the elementary components of cellular signaling transduction underlying leukocyte locomotion and endothelial cell activities [30, 31].

Migrated monocytes can differentiate into macrophages. Plasticity and flexibility are the key features of macrophages and reflect their activation states [32]. Activated macrophages have distinctive functional phenotypes that are similar to the Th1/Th2 polarization paradigm of T lymphocytes and can be defined as M1 and M2. M1 induced by Th1 signature cytokines [*e.g.*, interferon-γ (IFN-γ) and TNF-α], which are associated with the TLR-dependent signaling pathway, has the ability of up-regulating genes involved in cell-biased immunity, enhancing antigen

4

1 presentation, and producing a distinctive array of inflammatory cytokines (*e.g.*, IL-1β, IL-6,

2 and TNF-α). M2 induced by Th2 signature cytokines (*e.g.*, IL-4 and IL-13) plays an important

3 role in immune suppression, anti-inflammation (*e.g.*, IL-10), tissue regeneration, and wound

4 healing [*e.g.*, transforming growth factor-β (TGF-β) and vascular endothelial growth factor

5 (VEGF)] [33, 34].

6

7 The current study aimed to elucidate the exact mechanism of AgNPs-induced biological barrier

8 functional changes in the inner ear. We exposed the rat inner ear to AgNPs and hypothesized

9 that TLR signaling pathways were involved in AgNPs-induced hearing loss in association with

10 the potential recruitment of macrophages in the rat cochlea. A20 might play a role in regulating

11 the downstream signaling of TLR pathways. Molecules potentially involved in these signaling

12 pathways were thoroughly analysed using immunohistochemistry in the rat cochlea after

13 AgNPs exposure.

14

15 **Methods**

16 **Animal and AgNPs**

17 Ten albino male Sprague-Dawley rats weighing between 250 g and 300 g were kept at an am-

18 bient temperature of 20-22 °C with a relative humidity of 50±5 % under a 12/12 h light/dark

19 cycle in the experimental animal unit, University of Tampere. The experiments were performed

20 under general anaesthesia with a mixture of 0.5 mg/kg medetomidine hydrochloride (Domitor®,

21 Orion, Espoo, Finland) and 75 mg/kg ketamine hydrochloride (Ketalar®, Pfizer, Helsinki, Fin-

land) administered via intraperitoneal injection, followed by intramuscular injection of en-

rofloxacin (Baytril®vet, Orion, Turku, Finland) at a dose of 10 mg/kg to prevent potential in-

fection. The animals' eyes were protected by carbomer (Viscotears®, Novartis Healthcare A/S,

Denmark). All procedures in the study complied with local ethics committee standards (per-

mission number: ESAVI/3033/04.10.03/2011) and were conducted in accordance with Euro-

pean Legislation. The Ag NPs (Colorobbia, Firenze, Italy) used in this study were highly fac-

eted with a mean size of 21±8 nm using transmission electron microscope. The mean hydrody-

namic size of the particles was 117±24 nm when suspended in deionized water (dH$_2$O) using

dynamic light scattering, and the zeta potential was measured to be −20±9 mV [2]. More results

for the characterization could be referred to our previous study [2].

AgNPs administration

After anaesthetization, 40 μl of either 0.4 % (*n*=5) or 0.02 % (*n*=5) AgNPs were injected into

the middle ear cavity under an operating microscope (OPMI1-F, Carl Zeiss, Jena, Germany)

according to a previously reported procedure [1-3]. The tested concentrations were selected

according to the auditory brainstem response results showing that 0.4 % AgNPs caused reversi-

ble hearing loss that partially recovered at the 7th d, while 0.02 % AgNPs only induced hearing

loss at 32 kHz that returned to the baseline at the 7th d. Moreover, micro CT scanning displayed

that 0.4 % AgNPs caused an obvious middle ear infiltration that was absent in the rats exposed

to 0.02 % AgNPs [1-3]. The contralateral ear (*n*=10) received dH$_2$O under the same circum-

stances and was used as a negative control.

Sample preparation

On the 7th d post-injection, the anaesthetized rats were perfused with 0.01 M pH 7.4 phosphate buffered saline (PBS) containing 0.6 % (v/v) heparin (LEO Pharma A/S, Ballerup, Denmark) via a cardiac approach followed by 4 % paraformaldehyde (Merck, Espoo, Finland) to fix the head. The bullae were isolated after decapitation and decalcified using 10 % EDTA (Sigma, Steinheim, Germany) in the following 4 weeks with weekly solution changes. A standard procedure for paraffin embedding and tissue block was conducted in accordance with the protocol in a previous study [3].

Immunofluorescence staining

The procedure for immunofluorescence staining was in accordance with the protocol in a previous study [3]. The primary antibodies used in the assay were hosted in rabbit and were anti-CD68 (1:200, Abcam, UK), anti-CD44 (1:400, Abcam, UK), anti-TLR2 (1:250, Novus Biologicals, UK), anti-TLR4 (1:200, Novus Biologicals, UK), anti-MCP1 (1:4000, Novus Biologicals, UK), anti-MCP2 (1:200, GeneTex, USA), anti-Rac1 (1:800, Abcam, UK), anti-myosin light chain (1:100, Cell Signaling Technology, USA), anti-VCAM1 (1:50, Proteintech, USA), anti-Erk1/2 (1:400, Abcam, UK), anti-JNK (1:100, Cell Signaling Technology, USA), anti-p38 (1:100, Cell Signaling Technology, USA), anti-TNF-α (1:800, Abcam, UK), anti-TNFR1 (1:500, Abcam, UK), anti-TNFR2 (1:50, Abcam, UK), anti-IL-1β (1:400, Novus Biologicals, UK), anti-IL-10 (1:400, Abbiotec, USA), anti-TGF-β (1:500, Abcam, UK), anti-A20 (1:200, Sigma-Aldrich, USA), and anti-RNF11 (1:100, Abcam, UK). Briefly, the slices were incubated with the primary antibodies listed above at 4 °C overnight followed by Alexa Fluor® 488 Goat

7

1   Anti-Rabbit IgG (1:200, diluted with 0.1 % BSA, Life Technologies[TM], New York, USA) as a

2   secondary antibody at room temperature for 1 h in a dark environment. The nuclei were coun-

3   terstained with 10 μg/ml DAPI (Life Technologies[TM], New York, USA) at room temperature

4   for 10 min, and the slides were mounted for confocal microscopy with anti-quenching Fluoro-

5   mount (Sigma, St. Louis, USA). In the negative control slices, the primary antibodies were

6   replaced with 0.1 % BSA (dissolved in 0.01 M PBS pH 7.4, Sigma, St. Louis, USA).

7

Immunostaining visualized by 3, 3'-diaminobenzidine

9   After deparaffinization and hydration, the slices were immersed in 3 % H_2O_2-methanol at room

10 temperature for 30 min. After rinsing with PBS for 2×2 min, the slices were digested with 0.1 %

11 Trypsin (dissolved in 0.01 M PBS pH 7.4, Sigma, St. Louis, USA) at 37 °C for 30 min. After

12 rinsing with 0.1 % PBS-Tween® 20 (diluted in 0.01 M PBS pH 7.4, Sigma, St. Louis, USA) for

13 3×2 min, the slices were incubated with 10 % normal goat serum (Invitrogen, Paisley, UK) at

14 room temperature for 30 min followed by the primary antibodies listed above at 4 °C overnight.

15 After rinsing with 0.1 % PBS-Tween® 20 for 3×2 min, the slices were incubated with biotinyl-

16 ated goat anti-rabbit IgG at a dilution of 1:100 (Vector Laboratories Ltd., Peterborough, UK) at

17 room temperature for 1 h. After rinsing with 0.1 % PBS-Tween® 20 for 3×2 min, the slices were

18 incubated with the streptavidin-biotin-peroxidase complex (Vector Laboratories Ltd., Peterbor-

19 ough, UK) at 37 °C for 1 h. After rinsing with 0.1 % PBS-Tween® 20 for 3×5 min, antibody

20 binding was visualized by 3, 3'-diaminobenzidine using the DAB Peroxidase Substrate Kit

21 (Vector Laboratories Ltd., Peterborough, UK) at room temperature for 5 min. Alternatively, the

22 nuclei were counterstained using Harris's Solution (Merck, Darmstadt, Germany). Dehydration

1 and vitrification were completed by a standard protocol (70 % alcohol 10 s, 94 % alcohol 2×10

2 s, absolute alcohol 2×1 min, and xylene 3×3 min). The slides were mounted for light micros-

3 copy with Clarion™ Mounting Medium (Sigma, St. Louis, USA). Slices for negative controls

4 were prepared after the replacement of primary antibodies with 0.1 % BSA (dissolved in 0.01

5 M PBS pH 7.4, Sigma, St. Louis, USA). The staining intensities (shown by the greyscale value

6 that was inversely correlated with the staining intensity) in the strial basal cells, spiral ligament

7 fibrocytes, and spiral ganglion cells were measured and semi-quantified using ImageJ 1.45S

8 software (NIH, Bethesda, USA).

9

10 **Confocal and light microscopies**

11 The samples from immunofluorescence staining were observed and images obtained under a

12 Nikon microscope (ECLIPSE Ti) combined with an Andor confocal system installed with An-

13 dor iQ 2.8 software (Andor Technology, Belfast, UK). The excitation lasers were 405 nm (blue

14 excitation) and 488 nm (green excitation) from an Andor Laser Combiner System, and the cor-

15 responding emission filters were 450-465 nm (DAPI) and 525/50 nm (FITC), respectively. The

16 immunostained samples visualized by 3, 3'-diaminobenzidine were observed under a light mi-

17 croscope (LEICA DM 2000, Espoo, Finland), and images were digitally photographed using a

18 camera video (Olympus DP 25, Tokyo, Japan) with the cellSens Dimension 1.6 Olympus soft-

19 ware (Olympus Corporation, Tokyo, Japan) installed.

20

21 **Analysis and statistics**

1 Statistical analyses were performed using the IBM® SPSS® Statistics Version 20 software pack-

2 age (SPSS Inc., Chicago, USA). One-way ANOVA was used to compare the staining intensities

3 for CD68, TLR2, TLR4, MCP1, MCP2, A20, and RNF11 in the designated structures of differ-

4 ent cochlear turns among the cochleae exposed to 0.4 % AgNPs, 0.02 % AgNPs, and dH$_2$O.

5 The LSD *post-hoc* test was used to evaluate the pairwise difference. The independent sample *t*-

6 test was used to compare the staining intensities for CD44, Rac1, Erk1/2, IL-1β, IL-10, and

7 TGF-β in the designated structures of different cochlear turns between the cochleae exposed to

8 0.4 % AgNPs and dH$_2$O. A value of *p*<0.05 indicated that the difference was statistically sig-

9 nificant.

10

11 **Results**

12 **AgNPs augment the sensitivity and chemotactic proteins of cochlear cells**

13 In the cochleae exposed to dH$_2$O, the inner hair cells and pillar cells of Corti's organ showed

14 moderate staining for CD68, while the outer hair cells and Deiters' cells demonstrated extremely

15 weak staining for CD68 (Fig. 1H). The strial basal cells, spiral ligament fibrocytes, and spiral

16 ganglion cells exhibited mild staining for CD68 (Fig. 1D and 1F). In the cochlear lateral wall,

17 0.4 % AgNPs intensified CD68 staining remarkably in the strial basal cells (*p*<0.01, *post-hoc*

18 test) and spiral ligament fibrocytes (mainly Type III) (*p*<0.01, *post-hoc* test) in the 1st turn (Fig.

19 1A). However, no enhanced staining was observed in cells in the 2nd and 3rd turns (Fig. 1B and

20 1C) (*p*>0.05, *post-hoc* test). In the CD68+ cell population, sparse ramified cells and mononu-

21 clear cells were identified in the spiral ligament and the modiolus, respectively (Fig. 1C and 1I).

22 In Corti's organ, 0.4 % AgNPs increased CD68 staining in the inner hair cells and pillar cells

10

1 but not in the outer hair cells and Deiters' cells (Fig. 1G). In the spiral ganglion cells and capil-

2 lary endothelial cells, 0.4 % AgNPs did not alter CD68 staining in all turns (Fig. 1E) ($p>0.05$,

3 *post-hoc* test). 0.02 % AgNPs had no influence on CD68 staining in the aforementioned cells

4 in all turns (images not shown) ($p>0.05$, *post-hoc* test).

5

6 In the cochleae exposed to dH_2O, the strial intermediate cells, strial basal cells, spiral ligament

7 fibrocytes, spiral ganglion cells, and outer hair cells, pillar cells, and Deiters' cells of Corti's

8 organ showed intensive staining for CD44 (Fig. S1B, S1D, and S1F), while the inner hair cells

9 demonstrated mild staining for CD44 (Fig. S1F). 0.4 % AgNPs had no influence on the staining

10 in the aforementioned cells in all turns (Fig. S1A, S1C, and S1E) ($p>0.05$, independent sample

11 *t*-test).

12

13 In the cochleae exposed to dH_2O, the strial basal cells, spiral ligament fibrocytes (mainly Type

14 II), spiral ganglion cells, and inner hair cells and pillar cells of Corti's organ showed intensive

15 staining for TLR2 (Fig. S2B, S2D, and S2F), while the outer hair cells and Deiters' cells dis-

16 played extremely weak staining for TLR2 (Fig. S2F). The strial basal cells and spiral ligament

17 fibrocytes demonstrated mild staining for TLR4 (Fig. 2D), while the spiral ganglion cells and

18 hair cells, pillar cells, and Deiters' cells of Corti's organ exhibited extremely weak staining for

19 TLR4 (Fig. 2F and 2H). In the cochleae exposed to 0.4 % AgNPs, the outer hair cells and

20 Deiters' cells of Corti's organ showed more intensive staining for TLR2 (Fig. S2E). However,

21 the strial basal cells, spiral ligament fibrocytes, and spiral ganglion cells did not show any

22 changes in the staining of TLR2 in all turns (Fig. S2A and S2C) ($p>0.05$, one-way ANOVA),

11

1. nor in the inner hair cells and pillar cells (Fig. S2E). The strial basal cells ($p<0.05$ in the 1st and

2. 2nd turns and $p<0.01$ in the 3rd turn, one-way ANOVA) and spiral ligament fibrocytes (Fig. 2A-

3. 2C) ($p<0.05$ in the 1st, 2nd, and 3rd turns, one-way ANOVA) demonstrated more intensive stain-

4. ing for TLR4 that was independent of the cochlear turn ($p>0.05$, one-way ANOVA). The inner

5. hair cells, pillar cells, and Deiters' cells displayed more intensive staining for TLR4, but the

6. outer hair cells did not (Fig. 2G). However, the spiral ganglion cells did not show any changes

7. (Fig. 2E). 0.02 % AgNPs had no influence on the staining of TLR2 and TLR4 in the aforemen-

8. tioned cells in all turns (images not shown) ($p>0.05$, one-way ANOVA).

9.

10. In the cochleae exposed to dH$_2$O, the Deiters' cells of Corti's organ showed intensive staining

11. for MCP1, while the inner hair cells and inner pillar cells exhibited moderate staining for MCP1

12. (Fig. 3H). The strial intermediate cells, strial basal cells, spiral ganglion cells, outer hair cells,

13. and outer pillar cells demonstrated mild staining for MCP1 (Fig. 3D, 3F, and 3H), while the

14. spiral ligament fibrocytes displayed extremely weak staining for MCP1 (Fig. 3D). Unexpect-

15. edly, the strial basal cells, spiral ligament fibrocytes, spiral ganglion cells, and the hair cells,

16. pillar cells, and Deiters' cells of Corti's organ showed intensive staining for MCP2 (Fig. S3B,

17. S3D, and S3F). In the cochleae exposed to 0.4 % (Fig. 3A) and 0.02 % AgNPs (image not

18. shown), the strial intermediate cells, capillary endothelial cells, and strial basal cells ($p<0.01$,

19. one-way ANOVA) in the 1st turn demonstrated more intensive staining for MCP1. However,

20. the spiral ligament fibrocytes (mainly Type III) in the cochleae exposed to 0.4 % AgNPs (Fig.

21. 3A-3C) ($p<0.01$ in the 1st and 3rd turns and $p<0.05$ in the 2nd turn, one-way ANOVA) showed

22. more intensive staining for MCP1 that was independent of the cochlear turn ($p>0.05$, one-way

1 ANOVA). In addition, 0.4 % AgNPs increased MCP1 staining in the inner pillar cells and De-

2 iters' cells of Corti's organ (Fig. 3G). However, the spiral ganglion cells did not show any

3 changes (Fig. 3E) ($p>0.05$, one-way ANOVA). Neither 0.4 % nor 0.02 % AgNPs affected the

4 staining of MCP2 in the aforementioned cells in all turns (images not shown) ($p>0.05$, one-way

5 ANOVA).

6

7 AgNPs had no effect on the expressions of tight junction-associated proteins including

8 Rac1, myosin light chain, VCAM1, and MAPKs signaling proteins

9 In the cochleae exposed to dH$_2$O, the strial intermediate cells, strial basal cells, spiral ganglion

10 cells, and hair cells, pillar cells, and Deiters' cells of Corti's organ showed intensive staining for

11 Rac1 (Fig. S4B, S4D, and S4F), while the spiral ligament fibrocytes (mainly Type II) demon-

12 strated moderate staining for Rac1 (Fig. S4B). The spiral ganglion cells and inner pillar cells of

13 Corti's organ exhibited moderate staining for myosin light chain (Fig. S5D and S5F), while the

14 hair cells, outer pillar cells, and Deiters' cells displayed mild staining for myosin light chain

15 (Fig. S5F). The strial basal cells and spiral ligament fibrocytes showed extremely weak staining

16 for myosin light chain (Fig. S5B). The strial basal cells, spiral ligament fibrocytes, spiral gan-

17 glion cells, and hair cells, pillar cells, and Deiters' cells of Corti's organ showed extremely weak

18 staining for VCAM1 (Fig. S6B, S6D, and S6F), JNK (Fig. S8B, S8F, and S8J), and p38 (Fig.

19 S8D, S8H, and S8L). However, the strial intermediate cells, strial basal cells, spiral ligament

20 fibrocytes, spiral ganglion cells, and hair cells, pillar cells, and Deiters' cells of Corti's organ

21 showed intensive staining for Erk1/2 (Fig. S7B, S7D, and S7F). 0.4 % AgNPs had no influence

22 on the staining of Rac1 (Fig. S4A, S4C, and S4E) ($p>0.05$, independent sample t-test), myosin

13

1   light chain (Fig. S5A, S5C, and S5E), VCAM1 (Fig. S6A, S6C, and S6E), Erk1/2 (Fig. S7A,

2   S7C, and S7E) ($p>0.05$, independent sample t-test), JNK (Fig. S8A, S8E, and S8I), and p38

3   (Fig. S8C, S8G, and S8K) in the aforementioned cells in all turns.

4

5   AgNPs up-regulated the expressions of ubiquitin-editing proteins A20 and RNF11 without

6   affecting the expressions of inflammatory cytokines

7   In the cochleae exposed to dH_2O, the spiral ganglion cells, inner hair cells and inner pillar cells

8   of Corti's organ showed mild staining for TNF-α (Fig. S9H and S9N), while the strial basal

9   cells, spiral ligament fibrocytes, outer pillar cells, outer hair cells, and Deiters' cells demon-

10   strated extremely weak staining for TNF-α (Fig. S9B and S9N). The strial intermediate cells,

11   strial basal cells, and spiral ganglion cells exhibited mild staining for TNFR1 (Fig. S9D and

12   S9J), while the spiral ligament fibrocytes, hair cells, pillar cells, and Deiters' cells displayed

13   extremely weak staining for TNFR1 (Fig. S9D and S9P). The strial intermediate cells and strial

14   basal cells showed mild staining for TNFR2 (Fig. S9F), while the spiral ligament fibrocytes,

15   spiral ganglion cells, hair cells, pillar cells, and Deiters' cells demonstrated extremely weak

16   staining for TNFR2 (Fig. S9F, S9L, and S9R). The strial basal cells, spiral ganglion cells, and

17   pillar cells of Corti's organ exhibited intensive staining for IL-1β, while the spiral ligament

18   fibrocytes (mainly Type II) and inner hair cells displayed mild staining for IL-1β (Fig. S10B,

19   S10D, and S10F). The outer hair cells and Deiters' cells showed extremely weak staining for

20   IL-1β (Fig. S10F). 0.4 % AgNPs had no influence on the staining of TNF-α (Fig. S9A, S9G,

21   and S9M), TNFR1 (Fig. S9C, S9I, and S9O), TNFR2 (Fig. S9E, S9K, and S9Q), and IL-1β

22   (Fig. S10A, S10C, and S10E) ($p>0.05$, independent sample t-test) in the aforementioned cells

1   in all turns.

2

3   In the cochleae exposed to dH_2O, the spiral ganglion cells showed intensive staining for IL-10

4   (Fig. S11F), while the pillar cells of Corti's organ demonstrated mild staining for IL-10 (Fig.

5   S11J). The strial basal cells, spiral ligament fibrocytes, hair cells, and Deiters' cells exhibited

6   extremely weak staining for IL-10 (Fig. S11B and S11J). The spiral ganglion cells and pillar

7   cells of Corti's organ displayed intensive staining for TGF-β (Fig. S11H and S11L), while the

8   strial basal cells, spiral ligament fibrocytes, and inner hair cells demonstrated mild staining for

9   TGF-β (Fig. S11D and S11L). The outer hair cells and Deiters' cells showed extremely weak

10   staining for TGF-β (Fig. S11L). 0.4 % AgNPs had no influence on the staining of IL-10 (Fig.

11   S11A, S11E, and S11I) ($p>0.05$, independent sample t-test) and TGF-β (Fig. S11C, S11G, and

12   S11K) ($p>0.05$, independent sample t-test) in the aforementioned cells in all turns.

13

14   In the cochleae exposed to dH_2O, the spiral ganglion cells, inner hair cells, pillar cells, and

15   Deiters' cells of Corti's organ showed intensive staining for A20 (Fig. 4J and 4N), while the

16   strial basal cells, spiral ligament fibrocytes, and outer hair cells demonstrated mild staining for

17   A20 (Fig. 4D and 4N). The strial basal cells, spiral ganglion cells, and inner pillar cells of Corti's

18   organ exhibited intensive staining for RNF11, while the spiral ligament fibrocytes, hair cells,

19   and outer pillar cells displayed mild staining for RNF11 (Fig. 4H, 4L, and 4P). The Deiters'

20   cells showed extremely weak staining for RNF11 (Fig. 4P). In the cochlear lateral wall, 0.4 %

21   AgNPs enhanced the staining of A20 ($p<0.05$ in the 1st and 2nd turns and $p>0.05$ in the 3rd turn

22   at the strial basal cells, $p<0.05$ in the 1st and 3rd turns and $p<0.01$ in the 2nd turn at the spiral

15

1 ligament fibrocytes, one-way ANOVA) and RNF11 ($p>0.05$ in the 1st and 3rd turns and $p<0.05$

2 in the 2nd turn at the strial basal cells, $p<0.01$ in the 1st turn and $p<0.05$ in the 2nd and 3rd turns

3 at the spiral ligament fibrocytes, one-way ANOVA) remarkably in the strial basal cells and

4 spiral ligament fibrocytes that was independent of the cochlear turn (Fig. 4A-4C and 4E-4G)

5 ($p>0.05$, one-way ANOVA). In Corti's organ, 0.4 % AgNPs increased A20 staining in the outer

6 hair cells and Deiters' cells (Fig. 4M) and RNF11 staining in the outer pillar cells and Deiters'

7 cells (Fig. 4O). In the spiral ganglion cells and capillary endothelial cells, 0.4 % AgNPs did not

8 alter the staining of A20 and RNF11 in all turns (Fig. 4I and 4K) ($p>0.05$, *post-hoc* test). 0.02 %

9 AgNPs had no influence on the staining of A20 and RNF11 in the aforementioned cells in all

10 turns (images not shown) ($p>0.05$, *post-hoc* test).

11

12 The unchanged molecules in the rat cochlea exposed to AgNPs were summarized in Table 1.

13

14 **Table 1 Unchanged molecules in the rat cochlea exposed to AgNPs**

Functions/Properties	Molecules
Cell recruitment	CD44
Innate immunity	TLR2
Chemotaxis	MCP2
Tight junction-associated proteins	VCAM1, Rac1, and MLC[a]
Cellular signaling transduction	Erk1/2, JNK, and p38
Inflammation	IL-1β, TNF-α, TNFR1, TNFR2
Anti-inflammation	IL-10 and TGF-β

MLC^a: myosin light chain

Discussion

The current study showed that 0.4 % AgNPs but not 0.02 % AgNPs, up-regulated the expressions of CD68, TLR4, MCP1, A20, and RNF11 in the strial basal cells, spiral ligament fibrocytes, and non-sensory supporting cells of Corti's organ. 0.4 % AgNPs had no effect on CD44, TLR2, MCP2, Rac1, myosin light chain, VCAM1, Erk1/2, JNK, p38, IL-1β, TNF-α, TNFR1, TNFR2, IL-10, or TGF-β. The toxicological mechanism of AgNPs is unclear. The Ag$^+$ released from AgNPs was thought to be an important mediator involved in the pathological process associated with AgNPs exposure [35]. However, this is actually doubtful because no Ag$^+$ remains in either animal or human body after reacting with the Cl$^-$ and forming AgCl. The IC$_{50}$ for AgNO$_3$ was lower than that for AgNPs [1]. Our unpublished data demonstrated that AgCl did not cause any hearing loss at the 2nd d through the 7th d post-intratympanic injection at the saturated concentration (520 μg/100 g). Therefore, our hypothesis is that the cytokine alteration in the current study is resulted from intact AgNPs rather than the disassociated Ag$^+$.

Increasing evidence demonstrate that the inner ear is an active immune organ rather than an 'immunologically privileged organ' that was generally accepted previously [36]. Cochlear lateral wall including the stria vascularis and spiral ligament has been reported as the primary site harbouring macrophages in the inner ear of human and mouse [37, 38]. In the current study, cells that showed mild staining for CD68 without ramified morphology were identified in the

17

stria vascularis and spiral ligament of rat cochlea exposed to dH_2O, suggesting that the rat coch-

lea did not have typical tissue-resident macrophages and might have a different immune mech-

anism from the one in human. Macrophages were reportedly recruited into murine cochlea ex-

posed to noise and ototoxic drugs [39-42]. The current study detected a sparse appearance of

ramified CD68-positive cells in the spiral ligament and mononuclear cells in the modiolus of

cochlea exposed to 0.4 % AgNPs, implying that either the rat cochlea possessed a different

innate immune system from the mouse or the AgNPs triggered different signaling pathways

from noise and conventional ototoxic drugs. The sole up-regulation of MCP1 without sufficient

cooperation with other molecules such as CD44, Rac1, myosin light chain, and VCAM1 might

be the reason for failure in recruiting abundant macrophages into the cochlea [43-45]. Moreover,

the unchanged levels of Erk1/2, JNK, and p38 did not provide the molecular basis for the ad-

hesion and migration of monocytes [46]. Instead, the expressions of CD68 in the strial basal

cells, spiral ligament fibrocytes, and non-sensory supporting cells of Corti's organ were signif-

icantly up-regulated after 0.4 % AgNPs exposure.

The up-regulated CD68 might confer macrophage-like functions on the strial basal cells and

spiral ligament fibrocytes and enhance the immune activities of non-sensory supporting cells

of Corti's organ. Non-sensory supporting cells of Corti's organ are indicated as microglia-like

cells and may determine the fate of the auditory sensory epithelium because microglia are be-

lieved to be macrophages in the central nervous system and play an irreplaceable role in im-

mune surveillance [47-49]. CD68 was reportedly involved in vesicular trafficking to deliver the

lipids to their proper intracellular compartments [50]. The current study suggested that CD68

18

might be implicated in the activation of TLR4 via caveolae trafficking operated by lipid raft and caveolin-1 phosphorylation [51]. Previous research indicated that AgNPs induced the accumulation of hyaluronan, the substrate of TLR4, in the cochlea [3]. TLR4 was also up-regulated in the cochlea exposed to 0.4 % AgNPs in the current study. Theoretically, TLR4 activation triggers the NF-κB signaling pathway and finally up-regulates the expressions of inflammatory cytokines including IL-1β, TNF-α, and its receptors TNFR1 and TNFR2. However, neither the downstream cytokines of macrophages nor TLR4 activation was up-regulated in the cochlea exposed to AgNPs. Although it was unlikely that these pathways were never activated, it was predictable that certain cytokines were up-regulated at an early stage but suppressed afterwards. This possibility was supported by previous studies showing that AgNPs caused reversible changes to the permeability of biological barriers in the rat inner ear and transient hearing loss that partially recovered as of the 7th d [1, 3].

A20, in the context of RNF11, has been shown to inhibit TLR-mediated inflammatory response and its induced NF-κB signaling pathway [16, 17]. The current study showed that A20 and RNF11 were significantly up-regulated in the strial basal cells, spiral ligament fibrocytes, and non-sensory supporting cells of Corti's organ of cochlea exposed to 0.4 % AgNPs, suggesting that A20 and RNF11 might play roles in maintaining cochlear homeostasis and thus preserving hearing [1, 3]. However, the incomplete hearing recovery in the high-frequency range in the AgNPs-exposed ear suggested that the protective effects of A20 and RNF11 might be limited.

Conclusions

1 AgNPs might confer macrophage-like functions on the strial basal cells and spiral ligament

2 fibrocytes and enhance the immune activities of non-sensory supporting cells of Corti's organ

3 through the up-regulation of CD68, which might be involved in TLR4 activation. A20 and

4 RNF11 played roles in maintaining cochlear homeostasis via negative regulation of the expres-

5 sions of inflammatory cytokines. The current study suggested that the rat cochlea might have a

6 different immune mechanism from the one in human and mouse.

7

Abbreviations

9 AgNPs: silver nanoparticles; DAMP: danger/damage-associated molecular pattern; Erk1/2: ex-

10 tracellular signal-regulated kinases 1/2; IL-10: interleukin-10; IL-1β: interleukin-1β; JNK1/2/3:

11 c-Jun N-terminal kinases 1/2/3; MCPs: monocyte chemoattractant proteins; NF-κB: nuclear

12 factor-κB; PAMP: pathogen-associated molecular pattern; PRR: pattern recognition receptor;

13 RNF11: RING finger protein 11; SBCs: strial basal cells; SGCs: spiral ganglion cells; SLFs:

14 spiral ligament fibrocytes; TGF-β: transforming growth factor-β; TLR2/4: toll-like receptors

15 2/4; TNFRs: tumour necrosis factor receptors; TNF-α: tumour necrosis factor-α; VCAM1: vas-

16 cular cell adhesion molecule 1.

17

Competing interests

19 The authors declare that they have no conflict of interest.

20

Authors' contributions

22 Conceived and designed the experiments: JZ. Performed the experiments: HF. Analyzed the

20

data: HF and JZ. Wrote the paper: HF and JZ. Edited the paper: JZ and IP. All authors read and approved the final manuscript.

Authors' information

[1]Hearing and Balance Research Unit, Field of Oto-laryngology, School of Medicine, University of Tampere, Tampere, Finland. [2]Department of Otolaryngology-Head and Neck Surgery, Center for Otolaryngology-Head and Neck Surgery of Chinese PLA, Changhai Hospital, Second Military Medical University, Shanghai, China

References

1. Zou J, Feng H, Mannerstrom M, Heinonen T, Pyykko I. Toxicity of silver nanoparticle in rat ear and BALB/c 3T3 cell line. J Nanobiotechnology. 2014;12:52.

2. Zou J, Hannula M, Misra S, Feng H, Labrador RH, Aula AS, et al. Micro CT visualization of silver nanoparticles in the middle and inner ear of rat and transportation pathway after transtympanic injection. J Nanobiotechnology. 2015;13:5.

3. Feng H, Pyykko I, Zou J. Hyaluronan up-regulation is linked to renal dysfunction and hearing loss induced by silver nanoparticles. Eur Arch Otorhinolaryngol. 2015;272:2629-2642.

4. Termeer C, Benedix F, Sleeman J, Fieber C, Voith U, Ahrens T, et al. Oligosaccharides of Hyaluronan activate dendritic cells via toll-like receptor 4. J Exp Med. 2002;195:99-111.

5. Sloane JA, Batt C, Ma Y, Harris ZM, Trapp B, Vartanian T. Hyaluronan blocks oligodendrocyte progenitor maturation and remyelination through TLR2. Proc Natl Acad Sci U S A. 2010; 107:11555-11560.

6. Swaidani S, Cheng G, Lauer ME, Sharma M, Mikecz K, Hascall VC, et al. TSG-6 protein is crucial for the development of pulmonary hyaluronan deposition, eosinophilia, and airway hyperresponsiveness in a murine model of asthma. J Biol Chem. 2013;288:412-422.

7. Tolg C, McCarthy JB, Yazdani A, Turley EA. Hyaluronan and RHAMM in wound repair and the "cancerization" of stromal tissues. Biomed Res Int. 2014;2014:103923.

8. Elson G, Dunn-Siegrist I, Daubeuf B, Pugin J. Contribution of Toll-like receptors to the innate immune response to Gram-negative and Gram-positive bacteria. Blood. 2007;109:1574-1583.

9. Schmidt M, Raghavan B, Muller V, Vogl T, Fejer G, Tchaptchet S, et al. Crucial role for human Toll-like receptor 4 in the development of contact allergy to nickel. Nat Immunol. 2010; 11:814-819.

10. Jones BW, Means TK, Heldwein KA, Keen MA, Hill PJ, Belisle JT, et al. Different Toll-like receptor agonists induce distinct macrophage responses. J Leukoc Biol. 2001;69:1036-1044.

11. Castranova V. Signaling pathways controlling the production of inflammatory mediators in response to crystalline silica exposure: role of reactive oxygen/nitrogen species. Free Radic

Biol Med. 2004;37:916-925.

12. Zhou H, Zhao K, Li W, Yang N, Liu Y, Chen C, et al. The interactions between pristine graphene and macrophages and the production of cytokines/chemokines via TLR- and NF-kappaB-related signaling pathways. Biomaterials. 2012;33:6933-6942.

13. Lee EG, Boone DL, Chai S, Libby SL, Chien M, Lodolce JP, et al. Failure to regulate TNF-induced NF-kappaB and cell death responses in A20-deficient mice. Science. 2000;289:2350-2354.

14. Boone DL, Turer EE, Lee EG, Ahmad RC, Wheeler MT, Tsui C, et al. The ubiquitin-modifying enzyme A20 is required for termination of Toll-like receptor responses. Nat Immunol. 2004;5:1052-1060.

15. Liew FY, Xu D, Brint EK, O'Neill LA. Negative regulation of toll-like receptor-mediated immune responses. Nat Rev Immunol. 2005;5:446-458.

16. Gon Y, Asai Y, Hashimoto S, Mizumura K, Jibiki I, Machino T, et al. A20 inhibits toll-like receptor 2- and 4-mediated interleukin-8 synthesis in airway epithelial cells. Am J Respir Cell Mol Biol. 2004;31:330-336.

17. Guedes RP, Csizmadia E, Moll HP, Ma A, Ferran C, da Silva CG. A20 deficiency causes spontaneous neuroinflammation in mice. J Neuroinflammation. 2014;11:122.

18. Dalal NV, Pranski EL, Tansey MG, Lah JJ, Levey AI, Betarbet RS. RNF11 modulates microglia activation through NF-kappaB signalling cascade. Neurosci Lett. 2012;528:174-179.

19. Shembade N, Parvatiyar K, Harhaj NS, Harhaj EW. The ubiquitin-editing enzyme A20 requires RNF11 to downregulate NF-kappaB signalling. EMBO J. 2009;28:513-522.

20. Hollingsworth JW, Li Z, Brass DM, Garantziotis S, Timberlake SH, Kim A, et al. CD44 regulates macrophage recruitment to the lung in lipopolysaccharide-induced airway disease. Am J Respir Cell Mol Biol. 2007;37:248-253.

21. Beck-Schimmer B, Oertli B, Pasch T, Wuthrich RP. Hyaluronan induces monocyte chemoattractant protein-1 expression in renal tubular epithelial cells. J Am Soc Nephrol. 1998;9:2283-2290.

22. Deshmane SL, Kremlev S, Amini S, Sawaya BE. Monocyte chemoattractant protein-1 (MCP-1): an overview. J Interferon Cytokine Res. 2009;29:313-326.

23. Moon SK, Woo JI, Lee HY, Park R, Shimada J, Pan H, et al. Toll-like receptor 2-dependent

NF-kappaB activation is involved in nontypeable *Haemophilus influenzae*-induced monocyte chemotactic protein 1 up-regulation in the spiral ligament fibrocytes of the inner ear. Infect Immun. 2007;75:3361-3372.

24. Woo JI, Pan H, Oh S, Lim DJ, Moon SK. Spiral ligament fibrocyte-derived MCP-1/CCL2 contributes to inner ear inflammation secondary to nontypeable *H. influenzae*-induced otitis media. BMC Infect Dis. 2010;10:314.

25. Golias C, Tsoutsi E, Matziridis A, Makridis P, Batistatou A, Charalabopoulos K. Review. Leukocyte and endothelial cell adhesion molecules in inflammation focusing on inflammatory heart disease. In Vivo. 2007;21:757-769.

26. Cook-Mills JM. VCAM-1 signals during lymphocyte migration: role of reactive oxygen species. Mol Immunol. 2002;39:499-508.

27. Bruewer M, Hopkins AM, Hobert ME, Nusrat A, Madara JL. RhoA, Rac1, and Cdc42 exert distinct effects on epithelial barrier via selective structural and biochemical modulation of junctional proteins and F-actin. Am J Physiol Cell Physiol. 2004;287:C327-335.

28. Griffiths GS, Grundl M, Allen JS, 3rd, Matter ML. R-Ras interacts with filamin a to maintain endothelial barrier function. J Cell Physiol. 2011;226:2287-2296.

29. Tsukamoto O, Kitakaze M. Biochemical and physiological regulation of cardiac myocyte contraction by cardiac-specific myosin light chain kinase. Circ J. 2013;77:2218-2225.

30. Colombara M, Antonini V, Riviera AP, Mainiero F, Strippoli R, Merola M, et al. Constitutive activation of p38 and ERK1/2 MAPKs in epithelial cells of myasthenic thymus leads to IL-6 and RANTES overexpression: effects on survival and migration of peripheral T and B cells. J Immunol. 2005;175:7021-7028.

31. Cheng Q, Fan H, Ngo D, Beaulieu E, Leung P, Lo CY, et al. GILZ overexpression inhibits endothelial cell adhesive function through regulation of NF-kappaB and MAPK activity. J Immunol. 2013;191:424-433.

32. Mitchell AJ, Roediger B, Weninger W. Monocyte homeostasis and the plasticity of inflammatory monocytes. Cell Immunol. 2014;291:22-31.

33. Mills CD, Kincaid K, Alt JM, Heilman MJ, Hill AM. M-1/M-2 macrophages and the Th1/Th2 paradigm. J Immunol. 2000;164:6166-6173.

34. Mantovani A, Sica A, Sozzani S, Allavena P, Vecchi A, Locati M. The chemokine system

in diverse forms of macrophage activation and polarization. Trends Immunol. 2004;25:677-686.

35. Hadrup N, Lam HR. Oral toxicity of silver ions, silver nanoparticles and colloidal silver-a review. Regul Toxicol Pharmacol. 2014;68:1-7.

36. Harris JP, Tomiyama S. Experimental immune system of the inner ear. ORL J Otorhino-laryngol Relat Spec. 1987;49:225-233.

37. Zhang W, Dai M, Fridberger A, Hassan A, Degagne J, Neng L, et al. Perivascular-resident macrophage-like melanocytes in the inner ear are essential for the integrity of the intrastrial fluid-blood barrier. Proc Natl Acad Sci U S A. 2012;109:10388-10393.

38. O'Malley JT, Nadol JB, Jr. McKenna MJ. Anti CD163+, Iba1+, and CD68+ Cells in the Adult Human Inner Ear: Normal Distribution of an Unappreciated Class of Macrophages/Mi-croglia and Implications for Inflammatory Otopathology in Humans. Otol Neurotol. 2016;37: 99-108.

39. Hirose K, Discolo CM, Keasler JR, Ransohoff R. Mononuclear phagocytes migrate into the murine cochlea after acoustic trauma. J Comp Neurol. 2005;489:180-194.

40. Tornabene SV, Sato K, Pham L, Billings P, Keithley EM. Immune cell recruitment following acoustic trauma. Hear Res. 2006;222:115-124.

41. Sato E, Shick HE, Ransohoff RM, Hirose K. Expression of fractalkine receptor CX3CR1 on cochlear macrophages influences survival of hair cells following ototoxic injury. J Assoc Res Otolaryngol. 2010;11:223-234.

42. Hirose K, Li SZ, Ohlemiller KK, Ransohoff RM. Systemic lipopolysaccharide induces cochlear inflammation and exacerbates the synergistic ototoxicity of kanamycin and furo-semide. J Assoc Res Otolaryngol. 2014;15:555-570.

43. Matheny HE, Deem TL, Cook-Mills JM. Lymphocyte migration through monolayers of endothelial cell lines involves VCAM-1 signaling via endothelial cell NADPH oxidase. J Im-munol. 2000;164:6550-6559.

44. Sun C, Wu MH, Yuan SY. Nonmuscle myosin light-chain kinase deficiency attenuates ath-erosclerosis in apolipoprotein E-deficient mice via reduced endothelial barrier dysfunction and monocyte migration. Circulation. 2011;124:48-57.

45. Rom S, Fan S, Reichenbach N, Dykstra H, Ramirez SH, Persidsky Y. Glycogen synthase kinase 3beta inhibition prevents monocyte migration across brain endothelial cells via Rac1-

GTPase suppression and down-regulation of active integrin conformation. Am J Pathol. 2012;
181:1414-1425.

46. So H, Kim H, Lee JH, Park C, Kim Y, Kim E, et al. Cisplatin cytotoxicity of auditory cells
requires secretions of proinflammatory cytokines via activation of ERK and NF-kappaB. J As-
soc Res Otolaryngol. 2007;8:338-355.

47. Rio C, Dikkes P, Liberman MC, Corfas G. Glial fibrillary acidic protein expression and
promoter activity in the inner ear of developing and adult mice. J Comp Neurol. 2002;442:156-
162.

48. Ladrech S, Wang J, Simonneau L, Puel JL, Lenoir M. Macrophage contribution to the re-
sponse of the rat organ of Corti to amikacin. J Neurosci Res. 2007;85:1970-1979.

49. Sun S, Yu H, Yu H, Honglin M, Ni W, Zhang Y, et al. Inhibition of the activation and
recruitment of microglia-like cells protects against neomycin-induced ototoxicity. Mol Neuro-
biol. 2015;51:252-267.

50. Ashley JW, Shi Z, Zhao H, Li X, Kesterson RA, Feng X. Genetic ablation of CD68 results
in mice with increased bone and dysfunctional osteoclasts. PLoS One. 2011;6:e25838.

51. Jiao H, Zhang Y, Yan Z, Wang ZG, Liu G, Minshall RD, et al. Caveolin-1 Tyr14 phosphor-
ylation induces interaction with TLR4 in endothelial cells and mediates MyD88-dependent sig-
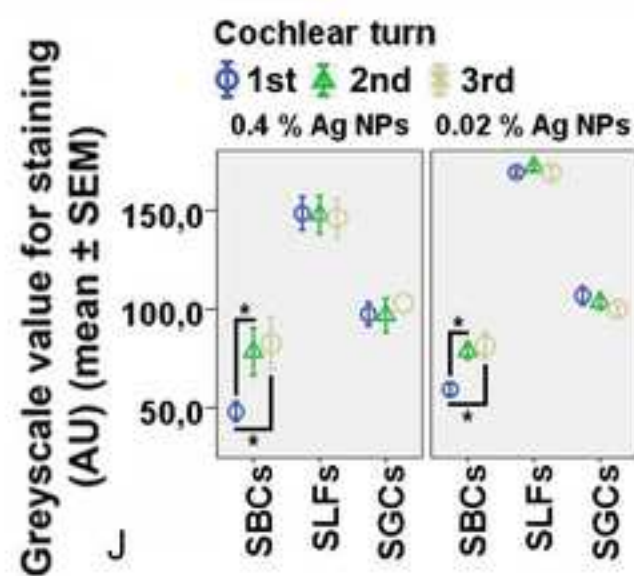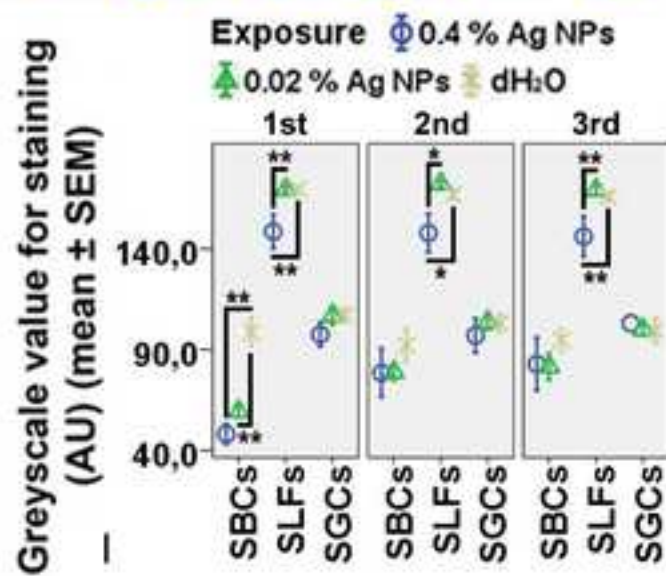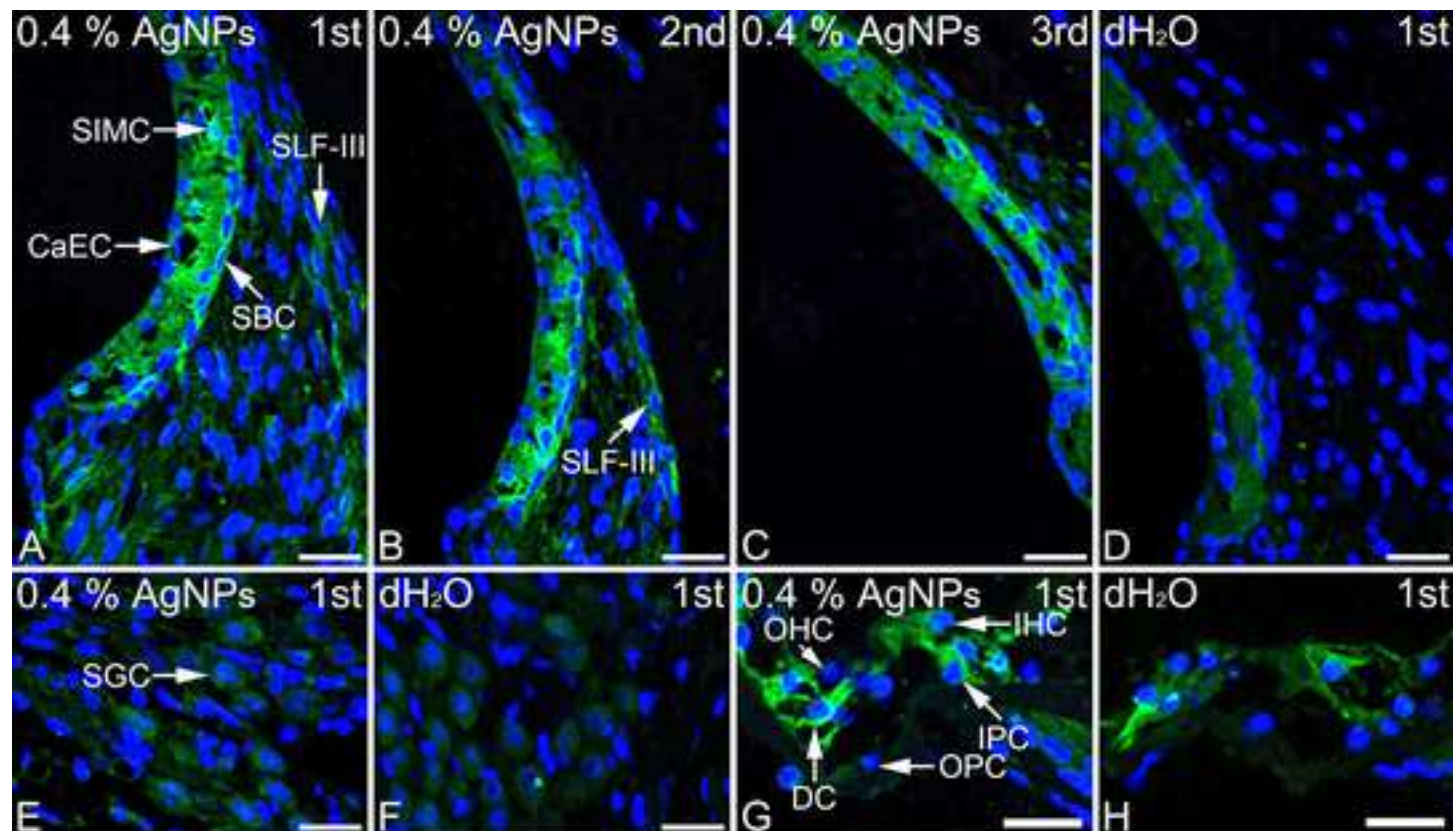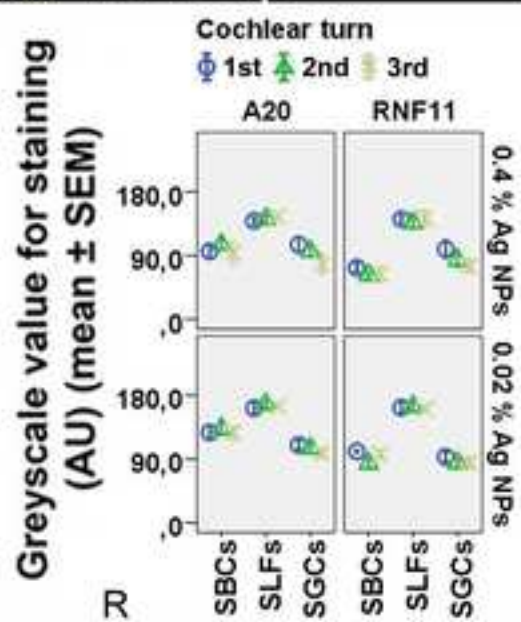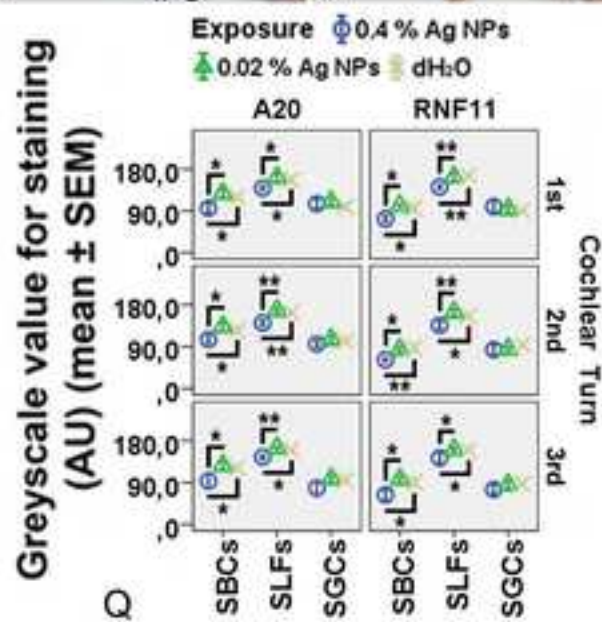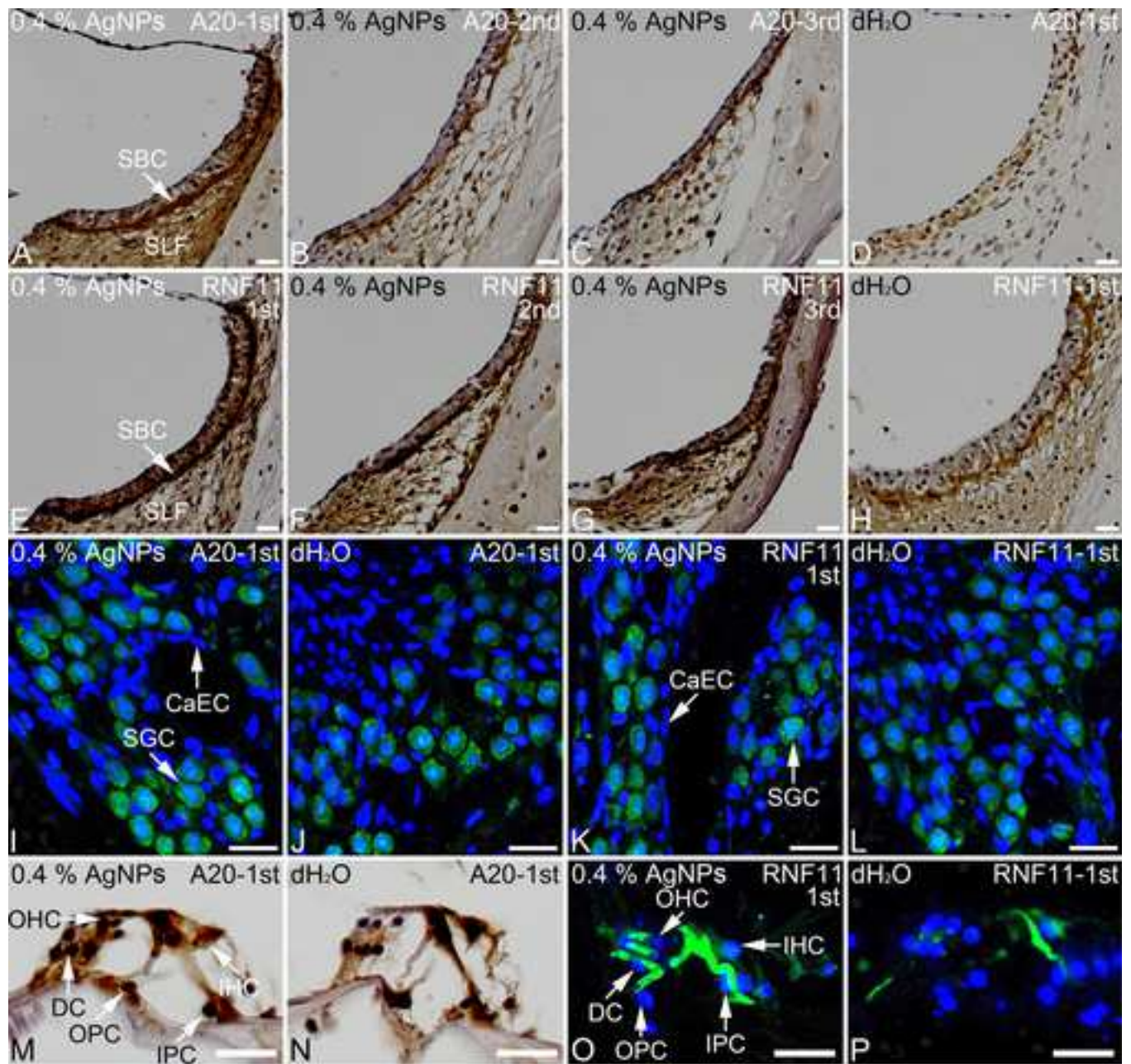naling and sepsis-induced lung inflammation. J Immunol. 2013;191:6191-6199.

Legend

Fig. 1 CD68^{+} cells in rat cochlea 7 d post-intratympanic injection of 0.4 % AgNPs shown by

immunofluorescence confocal microscopy or immunohistochemistry. In the cochleae exposed

to dH_2O, the inner hair cells (IHCs) and pillar cells (PCs) of Corti's organ (CO) showed mod-

erate staining, while the outer hair cells (OHCs) and Deiters' cells (DCs) demonstrated ex-

tremely weak staining (**H**). The strial basal cells (SBCs), spiral ligament fibrocytes (SLFs), and

spiral ganglion cells (SGCs) exhibited mild staining (**D** and **F**). In the cochleae exposed to 0.4 %

AgNPs, the SBCs and SLFs (mainly Type III) in the 1st turn (**A**) and the IHCs and PCs of CO

(**G**) displayed more intensive staining. Sparse ramified cells (**C**) and mononuclear cells (**I**) with

CD68 staining were identified in the spiral ligament and the modiolus, respectively. However,

the SBCs and SLFs in the 2nd and 3rd turns (**B** and **C**), SGCs (**E**), capillary endothelial cells

(CaECs) (**E**), OHCs, and DCs (**G**) did not show any changes. Comparisons of staining intensity

are shown in **J** and **K**. Scale bar = 30 μm in **A-F**, 20 μm in **G**, **H**, and the magnified image in **I**,

and 80 μm in **I**

Fig. 2 TLR4^{+} cells in rat cochlea 7 d post-intratympanic injection of 0.4 % AgNPs shown by

immunofluorescence confocal microscopy or immunohistochemistry. In the cochleae exposed

to dH_2O, the strial basal cells (SBCs) and spiral ligament fibrocytes (SLFs) showed mild stain-

ing (**D**), while the spiral ganglion cells (SGCs), hair cells (HCs), pillar cells (PCs), and Deiters'

cells (DCs) of Corti's organ (CO) demonstrated extremely weak staining (**F** and **H**). In the

cochleae exposed to 0.4 % AgNPs, the SBCs and SLFs exhibited more intensive staining that

was independent of the cochlear turn (**A-C**). In CO, the inner hair cells (IHCs), PCs, and DCs

1 displayed more intensive staining, but the outer hair cells (OHCs) did not (**G**). However, the

2 SGCs did not show any changes (**E**). Comparisons of staining intensity are shown in **I** and **J**.

3 Scale bar = 30 μm

4

5 **Fig. 3** MCP1^{+} cells in rat cochlea 7 d post-intratympanic injection of 0.4 % AgNPs shown by

6 immunofluorescence confocal microscopy or immunohistochemistry. In the cochleae exposed

7 to dH$_2$O, the Deiters' cells (DCs) of Corti's organ (CO) showed intensive staining, while the

8 inner hair cells (IHCs) and inner pillar cells (IPCs) exhibited moderate staining (**H**). The strial

9 intermediate cells (SIMCs), strial basal cells (SBCs), spiral ganglion cells (SGCs), and outer

10 hair cells (OHCs) and outer pillar cells (OPCs) of CO demonstrated mild staining, while the

11 spiral ligament fibrocytes (SLFs) displayed extremely weak staining (**D**, **F**, and **H**). In the coch-

12 leae exposed to 0.4 % AgNPs, the SLFs showed more intensive staining that was independent

13 of the cochlear turn, while the SIMCs, SBCs, and capillary endothelial cells (CaECs) demon-

14 strated more intensive staining in the 1st turn (**A**-**C**). In CO, the IPCs and DCs exhibited more

15 intensive staining, but the hair cells (HCs) and OPCs did not (**G**). However, the SGCs did not

16 show any changes (**E**). Comparisons of staining intensity are shown in **I** and **J**. Scale bar = 30

17 μm

18

19 **Fig. 4** A20[+] and RNF11^{+} cells in rat cochlea 7 d post-intratympanic injection of 0.4 % AgNPs

20 shown by immunofluorescence confocal microscopy or immunohistochemistry. In the cochleae

21 exposed to dH$_2$O, the spiral ganglion cells (SGCs), inner hair cells (IHCs), pillar cells (PCs),

22 and Deiters' cells (DCs) of Corti's organ (CO) showed intensive staining for A20 (**J** and **N**),

1   while the strial basal cells (SBCs), spiral ligament fibrocytes (SLFs), and outer hair cells (OHCs)

2   demonstrated mild staining for A20 (**D** and **N**). The SBCs, SGCs, and inner pillar cells (IPCs)

3   of CO exhibited intensive staining for RNF11, while the SLFs, hair cells (HCs), and outer pillar

4   cells (OPCs) displayed mild staining for RNF11 (**H**, **L**, and **P**). The DCs showed extremely

5   weak staining for RNF11 (**P**). In the cochleae exposed to 0.4 % AgNPs, the SBCs and SLFs

6   demonstrated more intensive staining for A20 and RNF11 that was independent of the cochlear

7   turn (**A**-**C** and **E**-**G**). In CO, the OHCs and DCs displayed more intensive staining for A20 (**M**),

8   the OPCs and DCs exhibited more intensive staining for RNF11 (**O**). However, the SGCs and

9   capillary endothelial cells (CaECs) did not show any changes in the staining of A20 and RNF11

10   (**I** and **K**). Comparisons of staining intensity are shown in **Q** and **R**. Scale bar = 50 μm in **A**-**H**,

11   20 μm in **M** and **N**, and 30 μm in **I**-**L**, **O**, and **P**

Figure_1

Click here to download Figure Figure_1.jpg

Figure_3

Click here to download Figure Figure_3.jpg ⬇

Figure_4

Click here to download Figure Figure_4.jpg ⬇
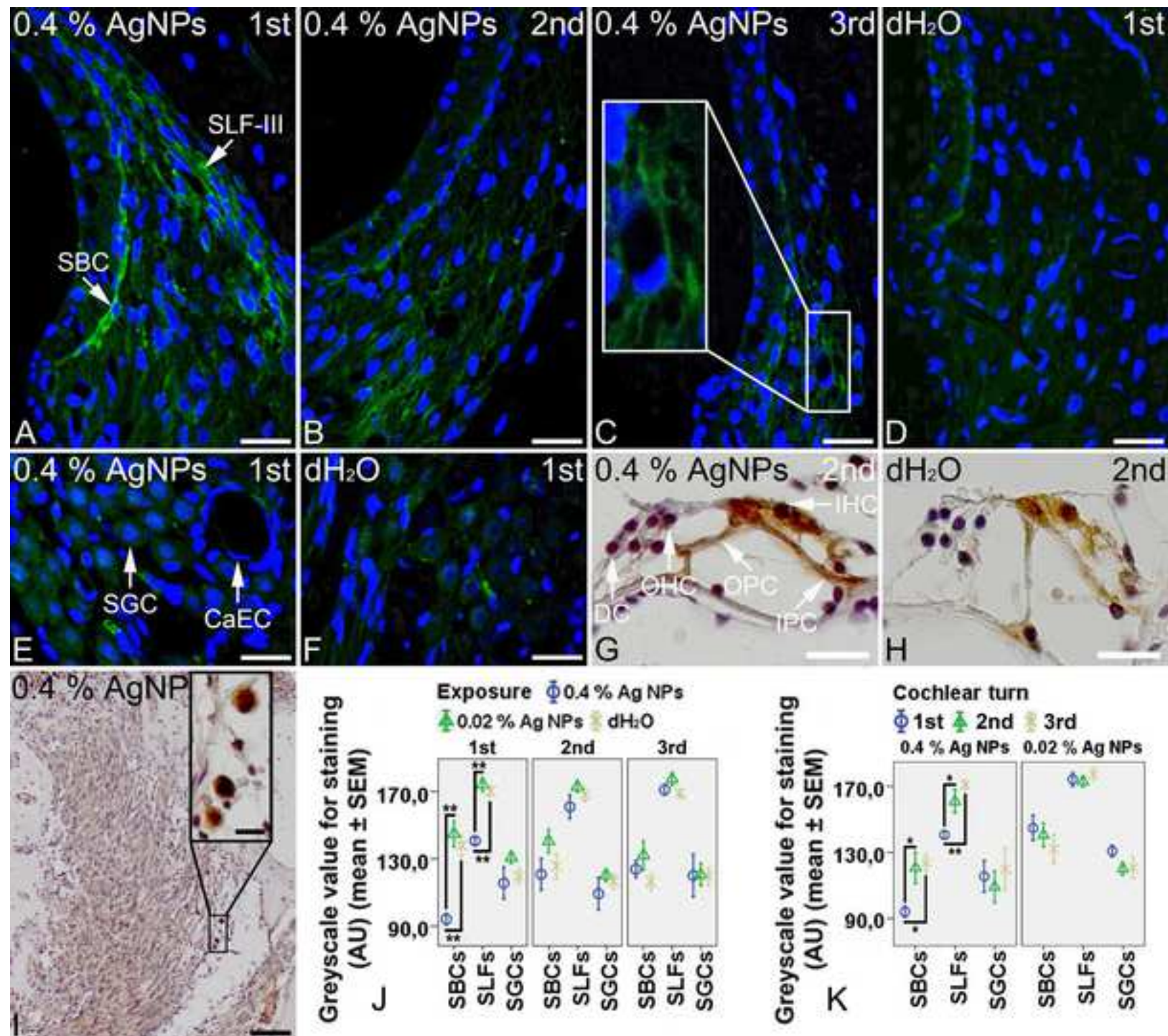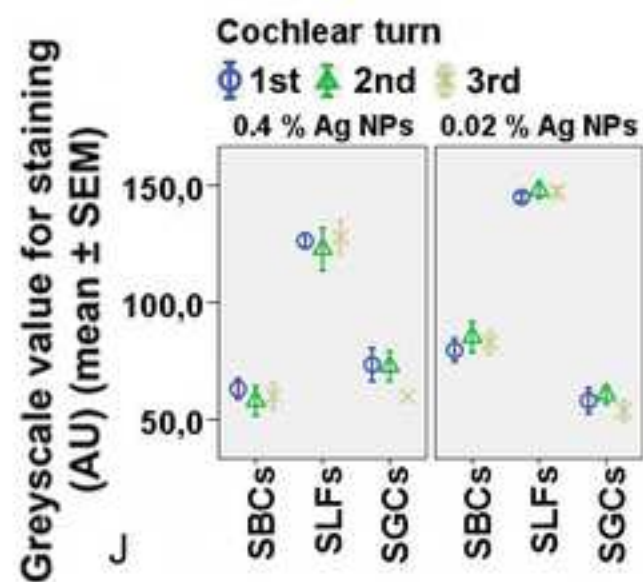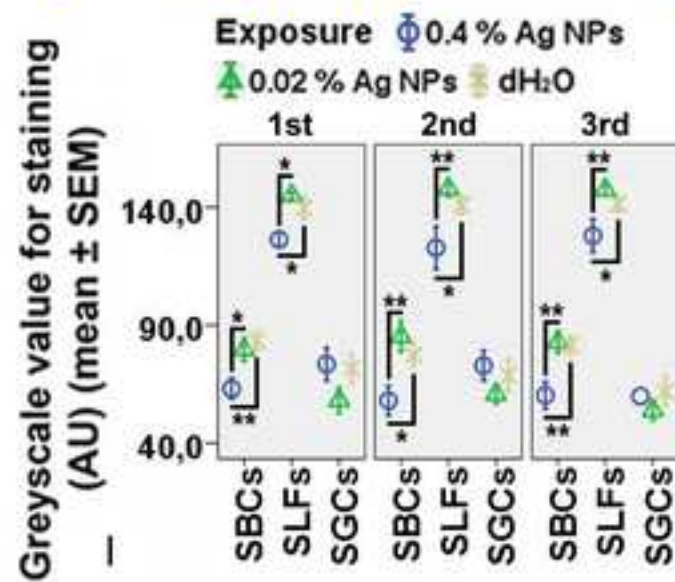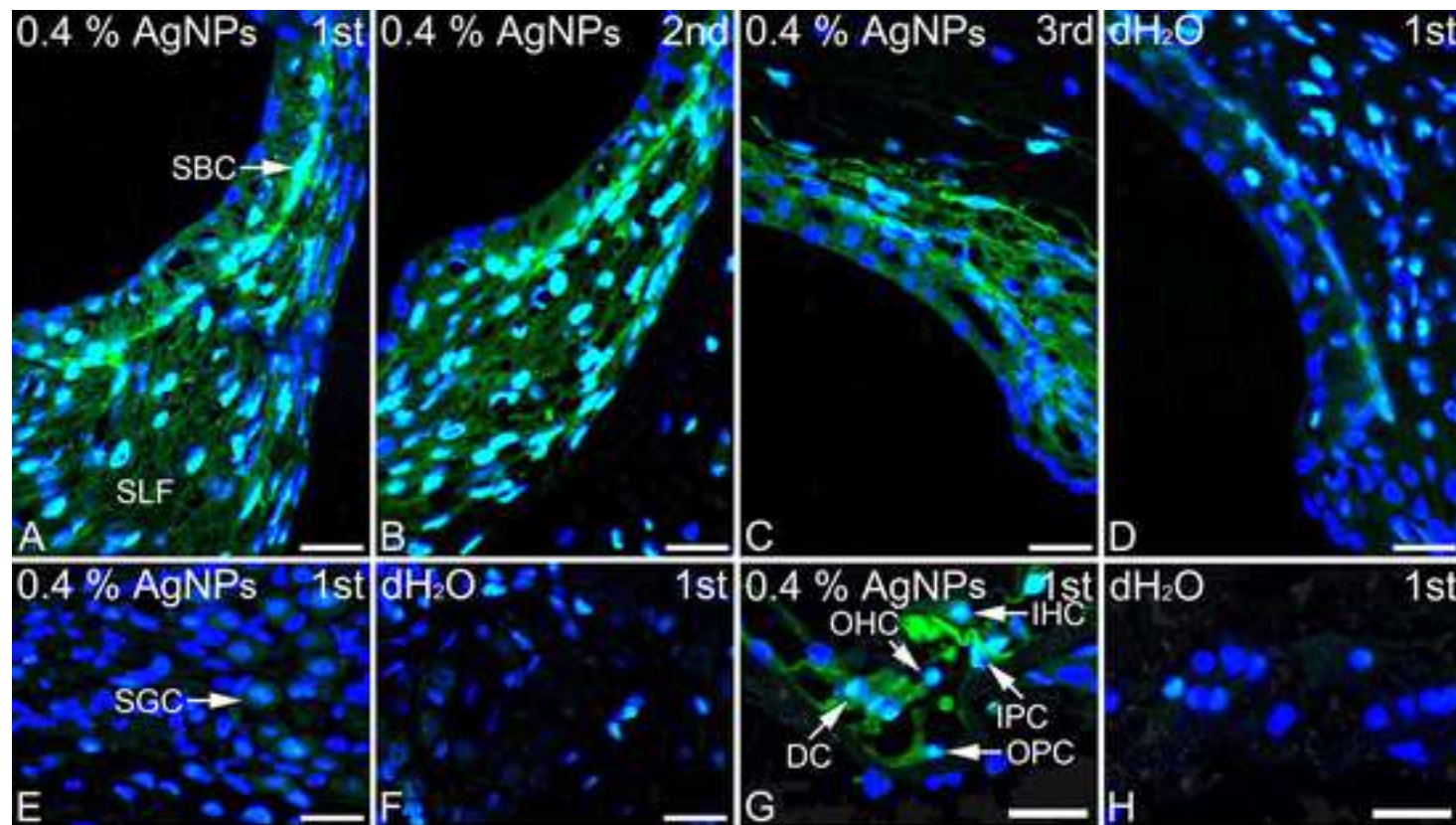
Click here to access/download
Supplementary Material
SFigure_1.jpg
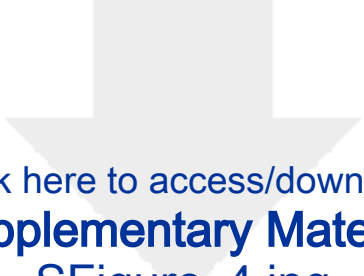
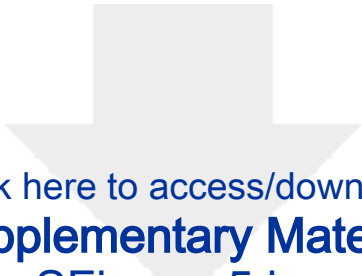Click here to access/download
Supplementary Material
SFigure_2.jpg
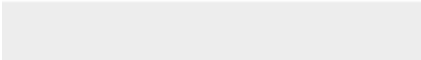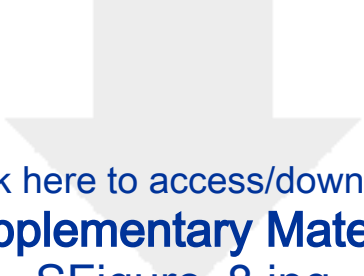
Click here to access/download
Supplementary Material
SFigure_3.jpg

Click here to access/download
Supplementary Material
SFigure_4.jpg

Click here to access/download
Supplementary Material
SFigure_5.jpg

Click here to access/download
Supplementary Material
SFigure_6.jpg

Click here to access/download
Supplementary Material
SFigure_7.jpg

Click here to access/download
Supplementary Material
SFigure_8.jpg

Click here to access/download
Supplementary Material
SFigure_9.jpg

Click here to access/download
Supplementary Material
SFigure_10.jpg

SFigure_11

Click here to access/download
Supplementary Material
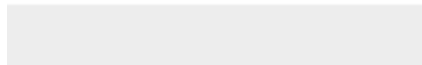SFigure_11.jpg

Click here to access/download
Supplementary Material
SFigure_12.jpg

Click here to access/download
Supplementary Material
Supplementary material-sent.docx

Ethical statement